AUTHOR and OTHER-AUTHOR

[Left hand page running head is author's name in Times New Roman 8 point bold capitals, centred. For more than two authors, write AUTHOR et al.]

CONFERENCE PRE-PRINT

CAN TURBULENT TRANSPORT IN OPTIMIZED STELLARATORS BE LOWER THAN TOKAMAKS?

Haotian Chen^{1,2}, Xishuo Wei², Hongxuan Zhu³, and Zhihong Lin^{2,*}

Abstract

Stellarators with three-dimensional (3D) magnetic configurations are attractive fusion reactor candidates due to their steady-state capability and inherent immunity to current-driven disruptions. Recent advances in optimized stellarator design have greatly reduced neoclassical transport and energetic-particle losses, motivating the need to assess turbulent transport and incorporate its optimization in reactor design. Turbulent transport driven by ion-temperature-gradient (ITG) and trapped-electron-mode (TEM) instabilities plays a dominant role in determining confinement properties. In this work, we perform global gyrokinetic GTC simulations of electrostatic ITG and TEM turbulence in several optimized stellarators —including quasi-axisymmetric (QA), quasi-helical (QH), and quasi-isodynamic (QI) configurations—as well as a reference tokamak based on the ITER steady-state scenario. The ITG-driven transport in QI and QH is comparable to that in the tokamak, while QA stellarators exhibit much higher transport under the same temperature gradient. Both ITG and TEM steady-state transport levels deviate significantly from quasi-linear predictions, with zonal-flow residuals and nonlinear saturation mechanisms playing key roles. These findings highlight the potential of optimized stellarators as viable reactor candidates and underscore the importance of controlling zonal-flow dynamics to minimize turbulent transport.

1. INTRODUCTION

Stellarators with 3-dimensional (3D) magnetic configurations are an attractive fusion reactor concept thanks to their steady state operation and reduced risk of disruptions since no plasma current drive is needed. With recent progress on optimized stellarator designs leading to drastically reduced neoclassical transport and energetic particle orbit loss, there is a pressing need to evaluate the turbulent transport in these stellarators and to incorporate optimization of turbulent transport in the reactor design. Turbulent transport caused by ion temperature gradient (ITG) instabilities play a major role in transport processes and strongly a ffect confinement properties. To be a competitive reactor candidate, the optimized stellarators need to demonstrate a turbulent transport level similar to or lower than an axisymmetric tokamak. Given the complexity of three-dimensional magnetic fields, global gyrokinetic simulations are crucial for determining the global ITG and TEM turbulent transport level and resulting confinement property in these optimized stellarators.

In this work we present global gyrokinetic GTC [1] simulations of electrostatic ITG and TEM turbulence in recently proposed quasi-axisymmetric (QA) stellarator [2], quasi-helical-symmetric (QH) stellarator [2], a compact QA design NCSX [3] in comparison with quasi-isodynamic (QI) stellarator model from W7-X [4] and axisymmetric tokamak model from ITER steady state scenario [5]. For ITG turbulence, we find that turbulent transport in QI and QH are comparable to tokamak, while QA stellarators have much higher transport with the same temperature or density gradient [6]. ITG steady state transport level can deviate significantly from quasi-linear scaling based on the linear growth rate. Further investigation shows zonal flow residual level and nonlinear stability play a crucial role in determining the nonlinear transport level. For TEM turbulence, the linear growth rates differ significantly among the optimized stellarators, with the QH configuration exhibiting the largest growth rate and the QA the smallest. Nonlinear simulations further reveal that the influence of zonal flows in TEM turbulence is qualitatively similar to that in ITG turbulence: the QA stellarator shows minimal turbulence suppression by zonal flows, whereas the QH configuration demonstrates the strongest zonal-flow regulation.

¹Fusion Simulation Center, Peking University, Beijing 100871, China

²Department of Physics and Astronomy, University of California, Irvine, CA 92697, USA

³Department of Astrophysical Sciences, Princeton University, Princeton, NJ 08544, USA

2. NONLINEAR ITG SIMULATION RESULTS

2.1. Simulation setups

In this study, global gyrokinetic simulations of ITG and TEM turbulence are performed for four optimized stellarator equilibria: a quasi-axisymmetric (QA) and a quasi-helically symmetric (QH) configuration recently optimized for neoclassical transport [2], a quasi-isodynamic (QI) configuration based on a W7-X model equilibrium [4], and a compact QA design (NCSX) optimized for ballooning stability [3]. For comparison, a model tokamak equilibrium corresponding to the ITER steady-state scenario [5] is also included.

All toroidal equilibria are computed using the VMEC code [6] and represented in Boozer coordinates (ψ, θ, ζ) , where ψ is the poloidal flux, θ the poloidal angle, and ζ the toroidal angle [7]. To ensure fair comparison of transport levels, all configurations are modeled with the same minor radius and temperature gradient. The minor radial coordinate is defined as $r = \sqrt{V/2\pi^2R}$, where R is the toroidally averaged major radius and $V(\psi)$ is the plasma volume enclosed by a flux surface labeled by ψ . The minor radius a is defined as $a = r(\psi_X)$ at the separatrix ψ_X . The ion and electron species are assumed to have equal temperatures, $T_i = T_e = T(r)$, with Maxwellian distributions and uniform density n. The temperature gradient is expressed by the inverse scale length, $L_T^{-1} = -dlnT/dr$. It is taken to be constant within the radial domain $r/a \in [0.3,0.8]$ and smoothly decreases to zero over a width of about 0.1a outside this region. All configurations have the same physical size, $a = 124\rho_s$, where $\rho_s = C_s/\Omega_i$ is the ion sound Larmor radius, Ω_i is the ion cyclotron frequency, $C_s = \sqrt{T_0/m_i}$ is the ion sound speed, m_i is the ion mass, and T_0 is the on-axis temperature.

2.2. Comparisons of turbulent transport levels

We first performed simulations with temperature gradient of $a/L_T=1.4$. The most striking result shown in FIG.1 (a) is that the heat conductivities χ_i are much higher than the QH and QI even though the linear growth rates and initial saturation levels are very similar in all stellarators. In the quasi-steady turbulence, the shearing rate ω_E is similar towards different stellarators. However, dure to the finite frequency zonal flows in QA, the effective shearing rate [8] ω_{Eff} of the QH and QI are much larger than the QA and tokamak, as shown in FIG. 1 (b). Consequently, the χ_i of the QH and QI is much smaller than QA and tokamak. These differences in transport and zonal flows are consistent and indicate different zonal flow dynamics in different magnetic configurations.

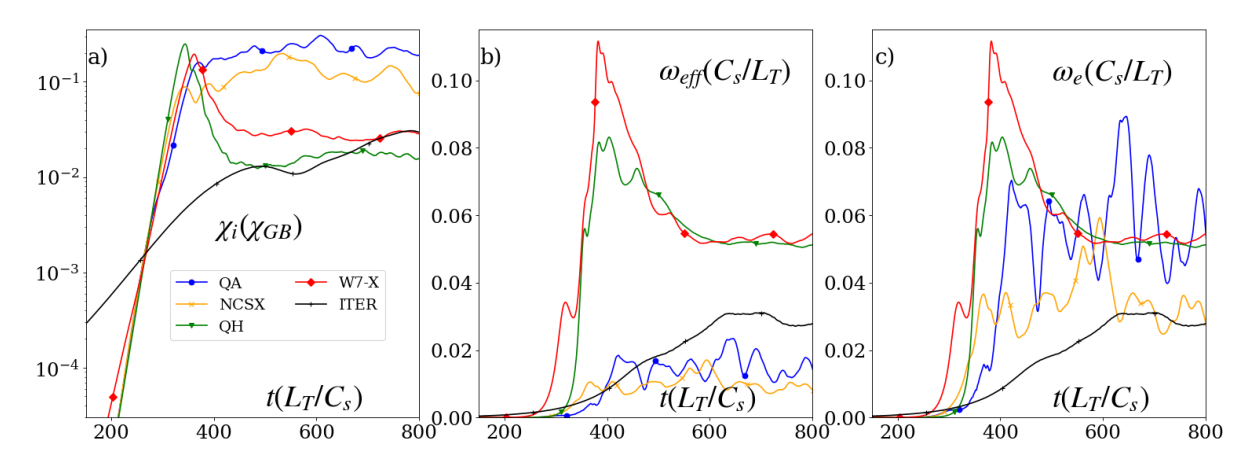


FIG. 1: Time history of heat conductivity χ_i (panel a) defined as $\chi_i \equiv QL_T/nT$ and is normalized to gyroBohm unit $\chi_{GB} \equiv \rho_s^2 C_s/L_T$ and zonal flow effective shearing rate [8] ω_{eff} (panel b) defined as $\omega_{eff} = \omega_E [(1+3F)^2+4F^3]^{1/4}/[(1+F)\sqrt{1+4F}]$ with $F \equiv \omega_{zf}^2/\Delta\omega_T^2$. ω_E (panel c) is the instantaneous shearing rate. ω_{zf} is the frequency of the zonal flow and $\Delta\omega_T$ is the decorrelation rate of the ambient turbulence.

2.3. Dynamics of zonal flows

To identify the reason of the difference in zonal flow dynamics. We plot in FIG.2 the time evolutions of the radial profiles of ion heat conductivities χ_i (left) and shearing rates ω_E (right). The zonal flows generated by turbulence are quickly damped to a residual level by the collisionless magnetic pumping effects [9]. This quasi-static zonal flow residual saturates the instability and suppresses the turbulent transport in the quasi-steady state. Linear GTC simulations [10] and gyrokinetic theory [11] find higher residual levels in the QH and QI than the QA and tokamak as shown in FIG. 2. The difference of zonal flow residual level thus can be considered in turbulence optimization in future stellarators.

Another important feature in FIG.2 is that the nonlinear frequency of zonal flows in the QA (and NCSX) is much higher than the QH and QI indicating a stronger nonlinear instability [12] of zonal flows in the QA. The higher frequency in the zonal flow diminishes its turbulence-suppression capability. In the QA configuration, although the instantaneous shearing rate is comparable to that in the QI and QH cases, the finite-frequency oscillation of the zonal flow lowers the effective shearing rate, thereby limiting its impact on turbulence regulation [8].

2.4. Transport scaling

To justify the finding a bove we observed is a universal effect across different profile gradients, we study the dependence of the transport levels and confinement times on the ITG instability drive by varying the temperature gradient. As shown in FIG. 3 (a), the linear ITG growth rates of the tokamak are much smaller than all the stellarators due to the larger Landau damping in Tokamak with smaller R_0/L_T . However, the ion heat conductivities χ_i of the tokamak are comparable to the QH and QI (panel b). On the other hand, the QA (and NCSX) heat conductivities are much larger. The QH and QI energy confinement times are comparable to the tokamak, while the QA energy confinement times are much shorter (panel c).

The reductions of heat conductivity χ_i^{nozf}/χ_i by zonal flows are shown in FIG. 3 (d). Here the heat conductivities χ_i^{nozf} are measured in simulations without zonal flows. We find that the reductions in the QH and QI are much bigger than the QA and tokamak. The turbulence suppression rate becomes smaller in QH with large temperature gradients. The reason is due the presence of finite frequency in zonal flows in simulation with large temperature gradients

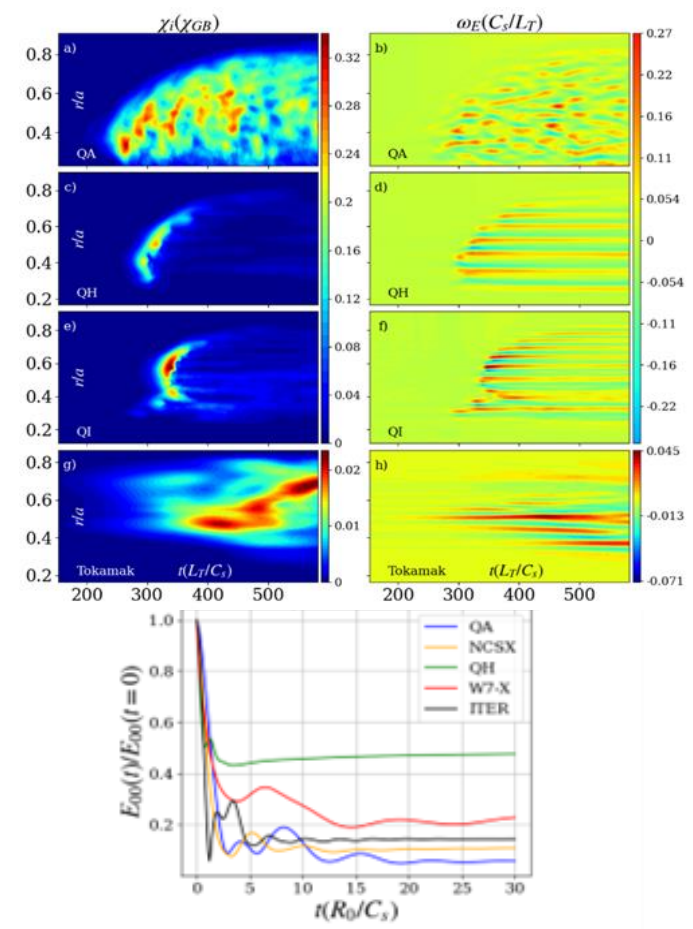


FIG.2: Time evolutions of the radial profiles of ion heat conductivities χ_i (left column) and zonal flow shearing rates ω_E (right column). The zonal flow damping test with finite wavelength (The dominant wavelength observed in turbulence simulation) is shown in panel I.

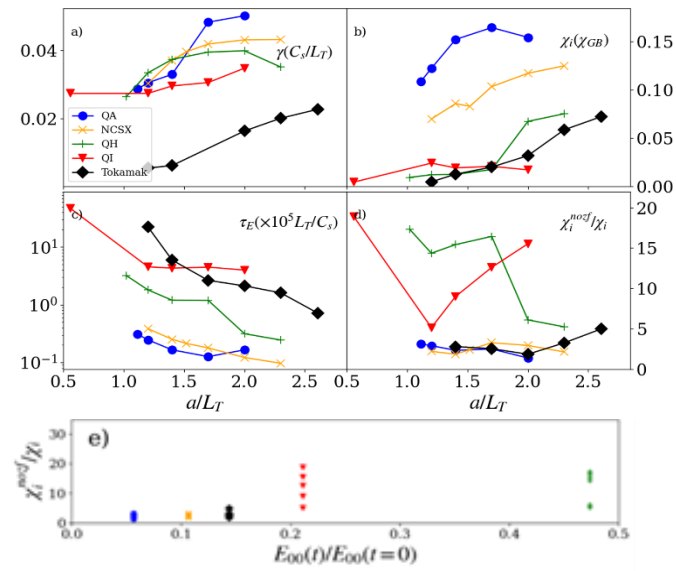


FIG. 3: Dependence of linear growth rates γ (panel a), heat conductivity χ_i (panel b), confinement times τ_E (panel c), and reduction by zonal flows (panel d) on temperature gradients.

3. NONLINEAR TEM DYNAMIC

We also simulate the TEM dynamics in all optimized stellarators. The TEM mode structures differ markedly from those observed in the ITG simulations as shown in FIG. 4. In the QA configuration, the TEM mode exhibits a more uniform distribution a cross toroidal angles, whereas in the QH configuration, it is strongly localized in the toroidal direction. This behaviour contrasts with the ITG case, where the QA mode is toroidally localized and the QH mode shows little isolation.

In the QI stellarator, the TEM mode structure shifts away from the outer midplane, which can be attributed to the misalignment between the trapped-particle region and the bad-curvature region [13]. In contrast, in the QS stellarator and the tokamak, the trapped-particle region largely coincides with the bad-curvature region, resulting in similar mode structures between the QS stellarator and tokamak, but pronounced differences when compared with the QI stellarator.

The linear growth rate of the TEM also exhibits a distinct trend compared with the ITG results, as shown in FIG. 5. In the ITG simulations, all stellarator configurations display comparable linear growth rates, whereas in the TEM simulations, the growth rates vary significantly among different geometries. This variation may originate from

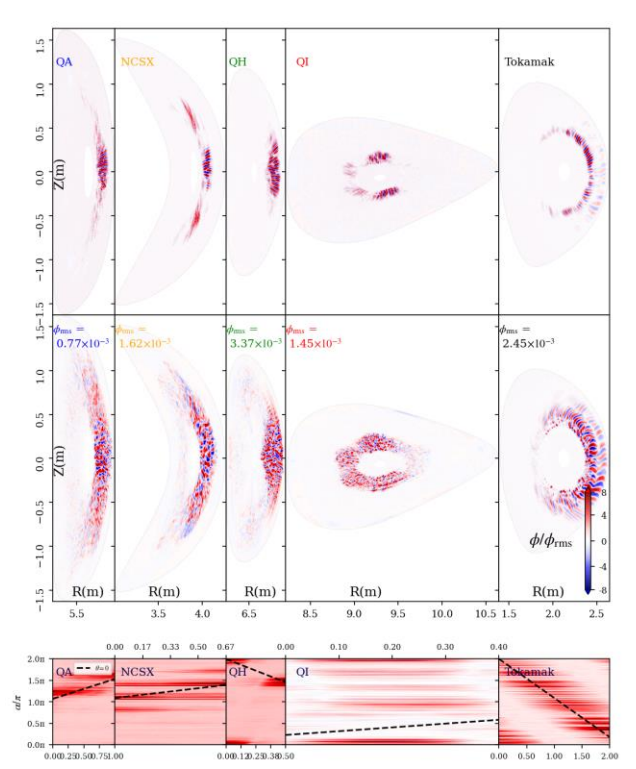


FIG. 4: The mode structure in linear and nonlinear stage of the TEM turbulence. The mode structure in the linear stage on one flux surface at the peak of the mode is shown in the bottom four panels

differences in the trapped-particle fraction and its spatial distribution inherent to each configuration, which warrants further investigation. In the nonlinear simulations, the zonal-flow dynamics show a trend similar to that observed in the ITG cases: the QH configuration exhibits strong turbulence suppression by zonal flows, while the QA configuration shows very weak suppression as shown in FIG. 6. Although the QH case reaches a higher fluctuation saturation level than NCSX, their overall nonlinear transport levels are comparable due to differences in the effectiveness of zonal-flow-mediated suppression.

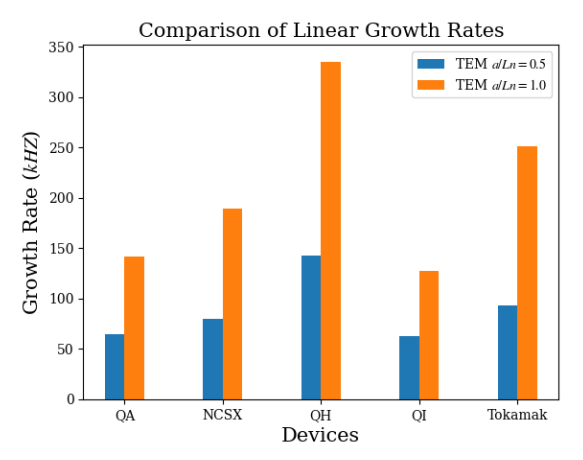


FIG. 5: The TEM linear growth rate in different devices with different density gradient $a/L_n = 0.5$ and $a/L_n = 1.0$.

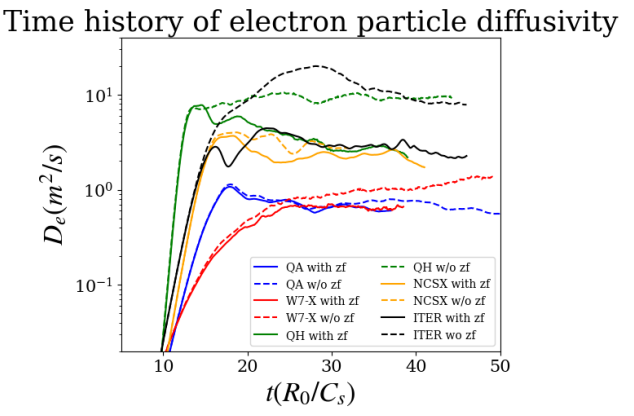


FIG. 6: The TEM linear growth rate in different devices with different density gradient $a/L_n = 0.5$ and $a/L_n = 1.0$.

AUTHOR and OTHER-AUTHOR

[Left hand page running head is author's name in Times New Roman 8 point bold capitals, centred. For more than two authors, write AUTHOR et al.]

4. CONCUSION AND FUTURE PLAN

The present global gyrokinetic simulations show that zonal flows lead to a much stronger reduction of ITG-driven transport in the QH and QI stellarators than in the QA stellarator or the tokamak. This enhanced suppression is attributed to higher linear residual levels and lower nonlinear oscillation frequencies of the zonal flows in the QH and QI configurations. As a result, the overall transport levels and energy confinement times in QH and QI are comparable to those in the tokamak with the same size and temperature gradient, despite the substantially larger linear growth rates in the stellarators.

For TEM turbulence, the linear properties vary significantly among devices, whereas the impact of zonal flows remains qualitatively similar. These results highlight a new pathway for improving plasma confinement by optimizing both the linear residual and nonlinear stability of zonal flows in stellarator design. The simulations suggest that, with further optimization of zonal-flow dynamics, turbulent transport in stellarators could ultimately fall below that in tokamaks.

Future work will extend these studies to include kinetic-electron and electromagnetic effects on confinement in optimized stella rators. Recently developed designs that minimize the linear ITG drive [13, 14] will be investigated as their equilibrium data become available. Moreover, we plan to explore zonal-flow optimization as a new design principle to reduce not only turbulent thermal transport, but also energetic-particle transport induced by Alfvén eigenmodes [15].

REFERENCES

- [1] Z. Lin et al, Science 281, 1835 (1998).
- [2] M. Landreman and E. Paul, Phys. Rev. Lett. 128, 035001 (2022).
- [3] O. P. Ford et al, Nucl. Fusion 64, 086067 (2024).
- [4] A. Reiman et al, Plasma Phys. Control. Fusion 41, B273 (1999).
- [5] A. R. Polevoi et al, Nucl. Fusion 60, 096024 (2020).
- [6] H. T. Chen, X. S. Wei, H. X. Zhu, and Z. Lin, Nucl. Fusion 65, 074002 (2025).
- [7] T. S. Hahm et al, Phys. Plasmas 6, 922 (1999).
- [8] G. G. Plunk and P. Helander, J. Plasma Phys. 90, 905900205 (2024).
- [9] J. H. Nicolau et al, Nucl. Fusion 61, 126041 (2021).
- [10] H. X. Zhu, Z. Lin, and A. Bhattacharjee, J. Plasma Phys. 91, E28 (2025).
- [11] P. H. Diamond et al, Plasma Phys. Control. Fusion 47, R35 (2005).
- [12] J. H. Nicolau, X. S. Wei, P. Liu, G. Choi, and Z. Lin, Nucl. Fusion 65, 086049 (2025).
- [13] A. G. Goodman et al, PRX Energy 3, 023010 (2024).
- [14] J. M. García-Regana et al, Nucl. Fusion 65, 016036 (2025).
- [15] P. Liu et al, Phys. Rev. Lett. 128, 185001 (2022).